Environ Res Tec, Vol. 8, Issue. 4, pp. 940-951, December 2025

Environmental Research and Technology
https://dergipark.org.tr/en/pub/ert
DOI:https://doi.org/10.35208/ert.1587144

Environmental Research & Technology

Research Article

Magnetic susceptibility and conductivity variations of Horseshoe Island (Antarctica): An indicator of environmental pollution vs lithological change

Murat ÖZKAPTAN[1*], Mert KAYA[1]

[1]*Karadeniz Technical University, Department of Geophysical Engineering, Trabzon-Türkiye*

ARTICLE INFO

Article history
Received: 18 November 2024
Revised: 14 January 2025
Accepted: 20 January 2025

Key words:
Magnetic susceptibility, conductivity, pollution, Horseshoe Island, Antarctica

ABSTRACT

Magnetic susceptibility and conductivity surveys are widely used to identify rock lithological changes, soil quality, and pollution (both atmospheric and human-related) due to their cost-effectiveness, energy efficiency, and simplicity. This study aims to determine the magnetic properties of igneous rocks, classified into five groups, on the northern side of Horseshoe Island (Antarctica). Rock samples were collected from 22 locations, covering five distinct lithologies. Measurements of magnetic susceptibility and conductivity were conducted at 1 cm vertical intervals, resulting in 828 recorded values. The data, analyzed at three levels (top, overall, and bottom), were used to differentiate between surface/atmospheric and mineralogical origins of the rocks. The results indicated that gabbro had the highest average susceptibility (3.91×10^{-3} CGS), while granitic gneiss showed zero susceptibility in all measurements. Conversely, granitic gneiss exhibited the highest conductivity values (116 S/m), whereas gabbro displayed the lowest conductivity (18.6 S/m). Spatially, susceptibility variations followed a northeast-southwest trend, particularly noticeable near the Turkish Scientific Station. High susceptibility was observed near Historical Site No. 63, while low values were concentrated around Gaul Cove. The findings highlight lithological differences, though snow and glacier cover limited precise boundary determinations. No significant differences were observed between surface and depth averages, suggesting mineral content influences exceed pollution effects.

Cite this article as: Özkaptan M, Kaya M. Magnetic susceptibility and conductivity variations of Horseshoe Island (Antarctica): An indicator of environmental pollution vs lithological change. Environ Res Tec 2025;8(4) 940-951.

INTRODUCTION

Environmental pollution, driven by multiple factors, pervades vast areas and disrupts the natural balance. Anthropogenic activities, such as the industrial revolution, world wars, and overpopulation, have posed significant threats to the environment, spreading their effects even to remote regions and reducing the quality of life [1, 2, 3]. Screening and detecting pollution have become increasingly important prerequisites for effective protection and remediation efforts. Heavy metals, fossil fuels, and chemical and biological wastes are among the most concerning pollutants in air, water, and soil.

Magnetic susceptibility and conductivity measurements are versatile tools frequently used to detect magnetic mineral concentrations and map polluted areas due to the high magnetic content of urban and industrial wastes containing heavy metals [4]. Conventional geochemical analyses for assessing heavy metal concentrations are often expensive and time-consuming, making magnetic measurements a practical alternative for detecting the composition, state, and grain

***Corresponding author.**
*E-mail address: ozkaptan@ktu.edu.tr

size of iron oxides, the most common ferrimagnetic minerals, and mapping their spatial distribution [5]. When iron oxide particles are discharged as pollutants, heavy metals may combine into their atomic lattice or adsorb onto their surfaces, leading to interrelated concentrations [6].

Rocks serve as natural repositories for various types of pollution. Advanced magnetic measurement techniques can detect the magnetic signals of even small fractions of ferromagnetic minerals, typically less than 1% [7]. Magnetic minerals in rocks can originate from lithogenic sources or form as secondary ferromagnetic materials due to anthropogenic activities [8, 9]. Anthropogenic dust particles, including magnetic minerals, accumulate on rocks, contributing to their magnetic signature. Magnetic methods are frequently used in shallow and deep crustal modelling studies [10, 11, 12]. Besides, numerous studies have explored rock magnetic mineralization and pollution-induced magnetization in different polluted environments [13, 14 15, 16, 17]. Anthropogenic pollution often exhibits a characteristic secondary magnetic signature, allowing magnetic surveys to distinguish pollution sources and monitor polluted areas [18].

This research focuses on pollution screening using magnetic susceptibility and conductivity analyses on Horseshoe Island, mid-latitude Antarctica. Although a limited number of magnetic and mineralogical studies have been conducted in the study area, these data were generally collected at very wide intervals and did not aim to reveal contaminant factors [19, 20, 21]. The primary aim is to demonstrate the applicability of environmental magnetic methods, especially in regions with relatively low polluting effects. Additionally, the study seeks to differentiate results arising from mineralogical and pollutant effects by comparing magnetic analysis results with rock lithology. Measurements from three different levels, from the surface to 10-30 cm depth, provide a clearer understanding of these effects.

MATERIALS AND METHODS

Study Area and Sampling

Horseshoe Island is located within the Marguerite Bay archipelago, along the west coast of the Antarctic Peninsula, West Antarctica (Figure 1a). The sampled area in the northwest of the island lies between latitudes 67.84°-67.78°S and longitudes 67.35°-67.15°W (Figure 1b). Covering a surface area of approximately 60 km², about 66% of the island is blanketed by glaciers or semi-permanent ice and snow [22, 23]. The island is divided into northern and southern sides by the Shoesmith Glacier. The complex and varied bedrock geology comprises mafic (gabbro and undifferentiated volcanic rocks) and felsic igneous rocks (brick-red, speckled, coarse pink, and heterogeneous granites) intruded in different phases, as well as metamorphic rocks (granitic gneiss) deformed under various metamorphic conditions [24], (Figure 2a). According to previous studies, the basement composed of Palaeozoic crystalline rocks and subduction-related Late Jurassic to Tertiary age volcanic rocks [25, 26, 27]. These rocks were deformed by gabbroic and granitic rocks as a result of Cretaceous to Eocene age magmatic intrusions [28].

Oriented hand samples were collected from 22 locations in the northern side of Horseshoe Island. The sampling sites included six locations for brick-red granite, seven for coarse pink granite, six for heterogeneous granite, two for gabbro, and one for granitic gneiss (Figure 2 and Table 1). Care was taken to distribute sampling sites homogeneously across the island and among different lithological units (Figure 2a). Directional samples of a minimum length of 15 cm were taken from the surface to compare the penetration effects of potential pollutants. The samples were wrapped in aluminium foil, sealed in plastic bags, and transported to the laboratory for magnetic measurements.

Measurements and Analysing

Field samples were prepared for magnetic analysis, maintaining their original orientation. Measurements were conducted vertically at 1 cm intervals from the highest to the lowest level of each sample (Figure 2d). Magnetic susceptibility and conductivity measurements were conducted at each level using a Terraplus KT-10 v2 susceptibility/conductivity meter. Magnetic susceptibility was measured at a single frequency of 10 kHz, ranging from 0.001×10^{-3} to 1999.99×10^{-3} SI with a sensitivity of 1×10^{-6} SI. Conductivity measurements were performed simultaneously, ranging from 1-100,000 S/m with a sensitivity of 1 S/m. These measurements were completed separately for two different sides of each rock sample (Table 1, Supplementary data).

Each data point was measured twice to ensure reproducibility and avoid errors. A total of 414 magnetic susceptibility and 414 conductivity measurements were conducted from the 22 rock samples. To account for drift, air readings were taken before and after each sample measurement series.

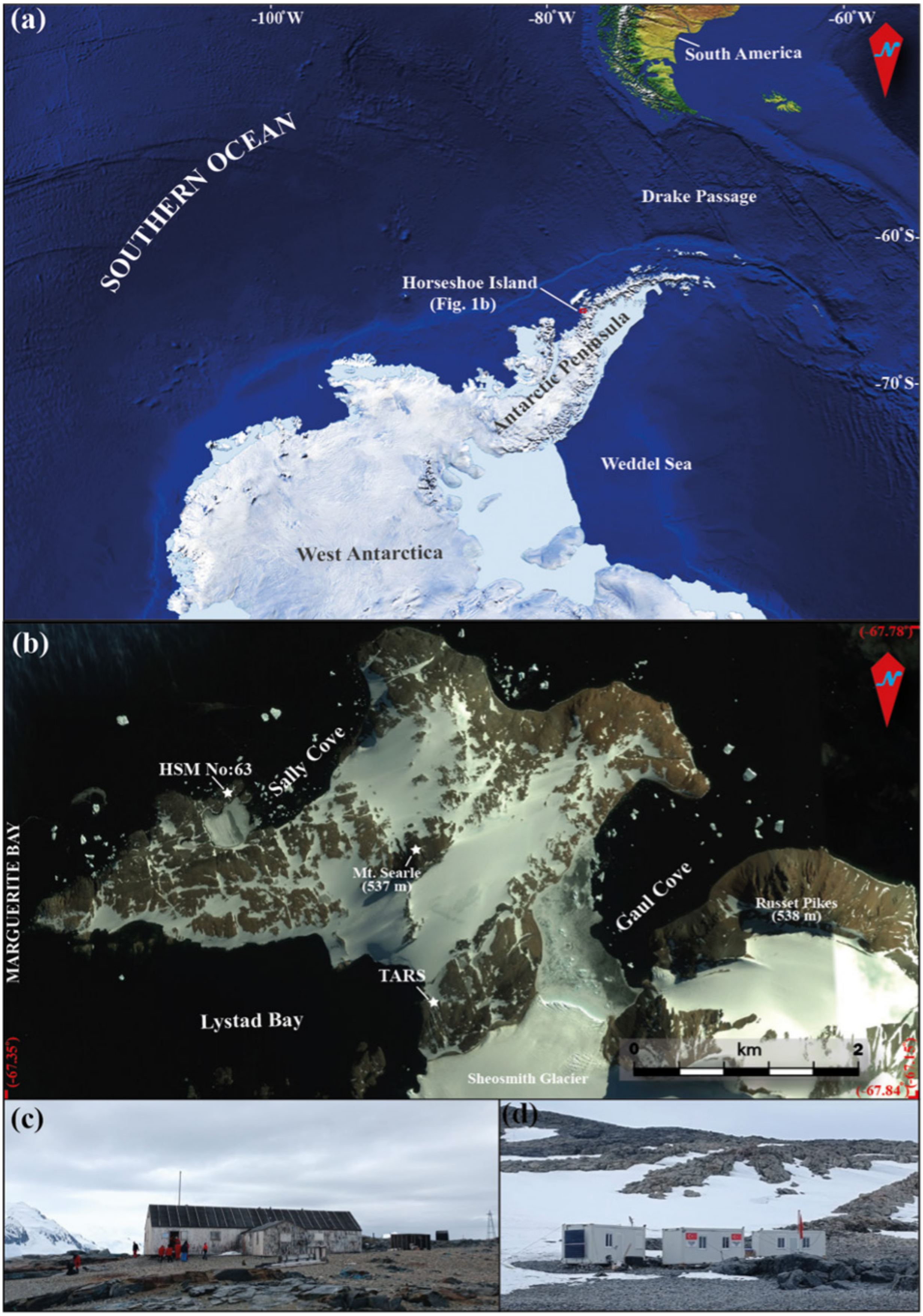

Figure 1. Location map of, a) circum-Antarctic Peninsula, and b) Northern side of the Horseshoe Island. c) HSM No:63 (Historical site No:63, British Former Scientific Station), d) TARS (Turkish Scientific Station)

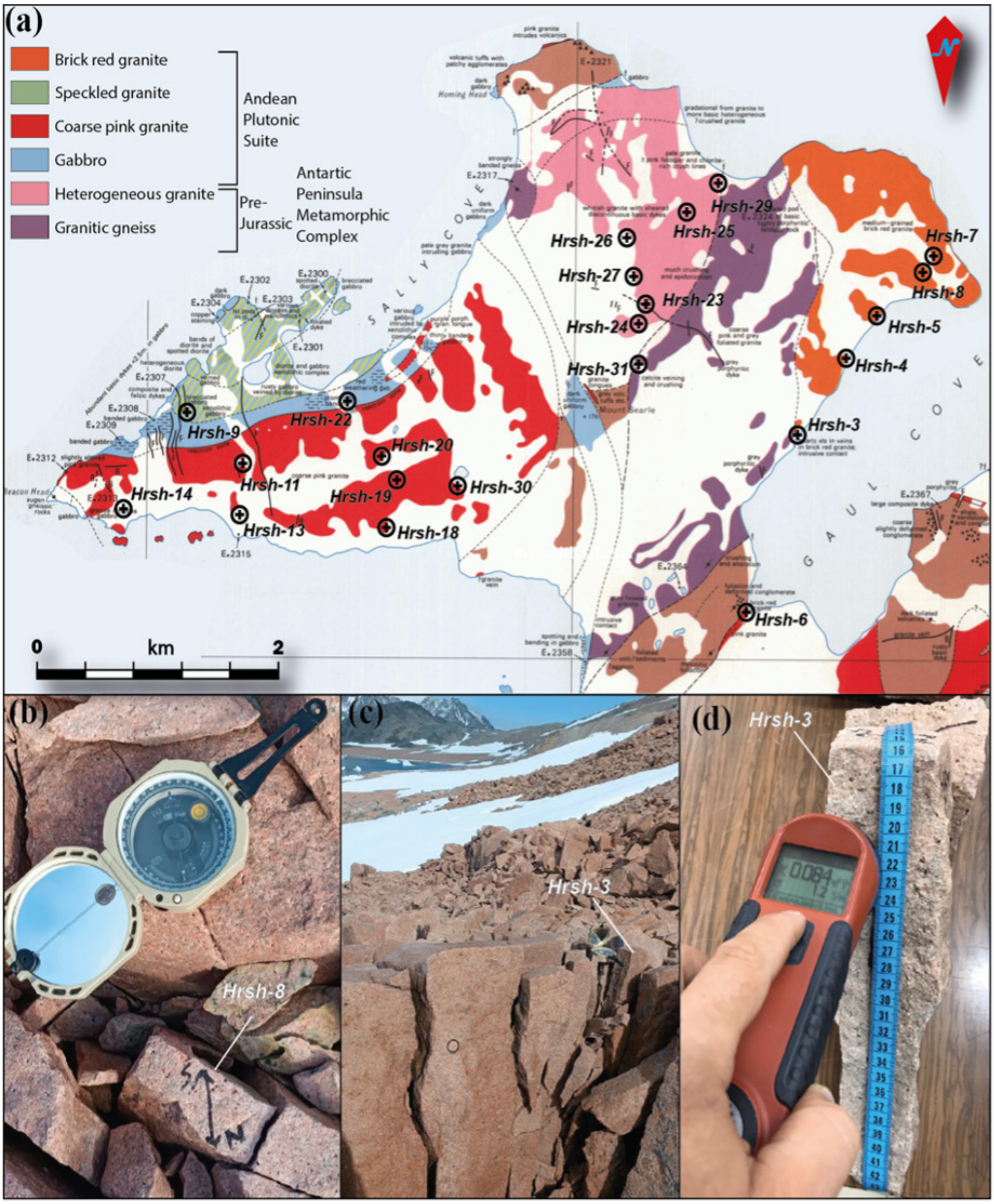

Figure 2. (a) Simplified geological map of the northern halve of the Horse Island (modified from Matthews 1983). (b) and (c) Photos showing the taking of oriented hand samples from the field. (d) Laboratory measurements (vertical) of hand samples from Horseshoe Island

RESULTS

The results of mean magnetic susceptibility and conductivity measurements are summarized in Table 1, which compares the values obtained from two sides of each rock sample. The "top" and "bottom" results represent the averages of the first and last five measurement values, respectively. The "mean" shows the average of all measured results in a sample. According to all average susceptibility results, the highest values were obtained from gabbro. This rock sampled in two locations shows clearly higher susceptibility values (8.25x10-3SI) compared to all other rock lithology. On the other hand, the lowest susceptibility averages were computed from brick red granites and heterogeneous granite (0x10-3SI). When the conductivity averages were compared according to lithology, the highest conductivity values were measured in granitic gneiss (164.6 S/m) and brick red granites (217 S/m), while the lowest value (or out of range) was found to be zero in gabbro (Table 1).

Table 1. Measured magnetic susceptibility and conductivity mean values from 22 rock samples collecting the study area

Site	Latitude	Longitude	Lithology	(side-1) Susceptibility (10-3) SI top/mean/bottom	(side-1) Conductivity SI top/mean/bottom	(side-2) Susceptibility (10-3) SI top/mean/bottom	(side-2) Conductivity SI top/mean/bottom
Hrsh-3	-67.815283°	-67.198780°	Brick-red granite	0.13/0.09/0.03	62.96/79.57/87.06	0.05/0.04/0.07	60.66/84.01/93.88
Hrsh-4	-67.811495°	-67.190818°	Brick-red granite	0.19/0.18/0.17	41.82/33.96/26.02	0.15/0.15/0.14	36.24/31.13/26.26
Hrsh-5	-67.810033°	-67.186462°	Brick-red granite	0.16/0.21/0.22	162/80.82/33.26	0.16/0.2/0.18	82.16/42.98/18
Hrsh-6	-67.828652°	-67.207905°	Brick-red granite	0.55/0.6/0.65	45.9/43.43/40.97	0.49/0.46/0.44	51.53/46.33/41.13
Hrsh-7	-67.803527°	-67.171662°	Brick-red granite	0.01/0.01/0	190.75/178.5/166.25	0/0/0	217.25/205.25/193.25
Hrsh-8	-67.804148°	-67.173288°	Brick-red granite	0/0/0	62.93/60.08/57.23	0/0/0	38.57/42.2/45.83
Hrsh-9	-67.812682°	-67.314668°	Gabbro	2.59/2.62/2.53	67.4/27.84/0.48	2.18/2.08/1.71	40.14/23.72/20.68
Hrsh-11	-67.817323°	-67.312877°	Coarse pink granite	0.73/0.7/0.67	161.4/150.8/140.2	0.67/0.65/0.62	150.6/151.4/152.2
Hrsh-13	-67.819040°	-67.313237°	Coarse pink granite	1.13/1.13/1.13	71.2/71.2/71.2	0.95/0.95/0.95	53.64/53.64/53.64
Hrsh-14	-67.819098°	-67.327443°	Coarse pink granite	1.23/1.17/1.11	44.3/37.3/30.3	1.25/1.15/1.06	55.37/35.67/15.97
Hrsh-18	-67.822123°	-67.281022°	Coarse pink granite	0.18/0.18/0.18	159/159/159	0.07/0.07/0.07	153.6/153.6/153.6
Hrsh-19	-67.818715°	-67.283547°	Coarse pink granite	0.44/0.39/0.32	87.2/76.46/61.17	0.51/0.47/0.39	61.1/56.5/53.73
Hrsh-20	-67.815970°	-67.291297°	Coarse pink granite	1.54/1.39/1.23	94.3/113.48/132.67	1.3/1.27/1.2	75.83/90.04/108.3
Hrsh-22	-67.814367°	-67.288570°	Gabbro	8.25/8.25/8.25	0/0/0	7.73/7.73/7.73	0/0/0
Hrsh-23	-67.808943°	-67.227295°	Heterogeneous granite	1.17/1.2/1.13	46.08/59.4/72.86	0.87/0.93/0.98	103.84/82.49/63.68
Hrsh-24	-67.808537°	-67.226123°	Heterogeneous granite	1.67/1.6/1.45	42.52/56.55/75.13	1.65/1.5/1.33	33.27/59.43/90.63
Hrsh-25	-67.801352°	-67.218782°	Heterogeneous granite	1.46/1.33/1.2	17.5/28.3/39.1	0.9/0.82/0.6	7.13/21.59/42.6
Hrsh-26	-67.802095°	-67.228305°	Heterogeneous granite	0/0/0	24.2/34.5/45.83	0.04/0.05/0.05	28.3/35.09/40.77
Hrsh-27	-67.804358°	-67.228052°	Heterogeneous granite	0.88/0.82/0.77	27.94/21.87/17.98	1.07/0.86/0.63	0.7/6.07/12.66
Hrsh-29	-67.798338°	-67.210953°	Heterogeneous granite	1.34/1.36/1.3	7.53/10.17/15.35	1.64/1.6/1.39	13.28/46.02/89.6
Hrsh-30	-67.820007°	-67.262200°	Coarse pink granite	2.65/1.59/0.67	0/9.89/17.43	0.79/0.84/0.86	3.18/6.16/10.68
Hrsh-31	-67.810772°	-67.225983°	Granitic gneiss	0/0/0	91/102.88/117.44	0/0/0	105.82/129.34/164.6

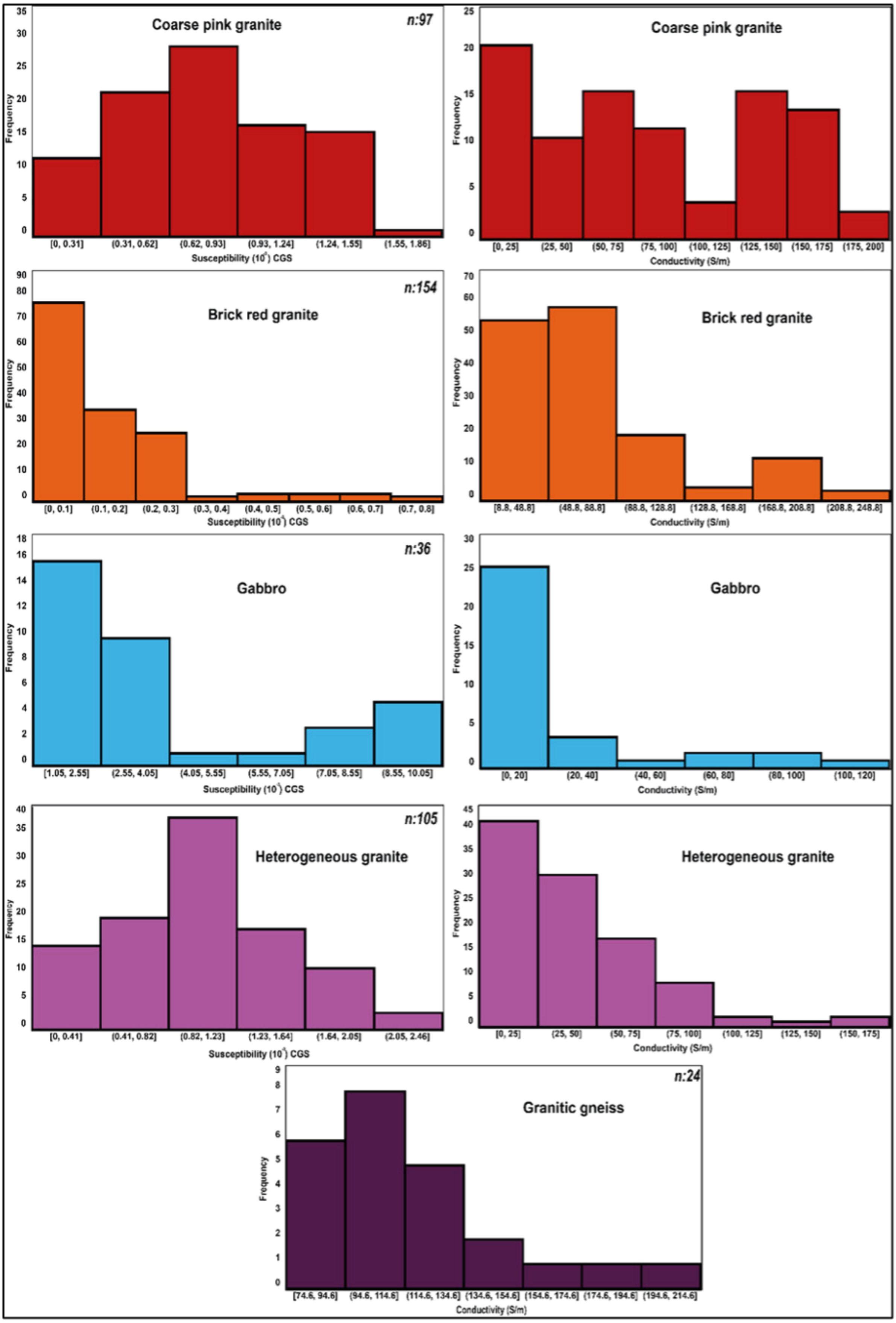

Figure 3. Magnetic susceptibility and conductivity histograms of five different rock lithology. n: number of measurements

As a measurement strategy, when the values taken from top to bottom for all rock samples were compared among themselves, no significant difference was obtained for susceptibility and conductivity results. The differences for the top and bottom are generally less than 10%. Moreover, there are no significant variances in comparing the results both susceptibility and conductivity measurements from two different faces of rock samples (Table 1). Related illustrations of these analyses are given in the discussions section.

Histograms of magnetic susceptibility and conductivity results versus lithological variances are illustrated in Figure 3. In general, the results obtained are far from normal distribution due to the insufficient number of measurements or the complexity of the mineral composition within the rock. Only the susceptibility results obtained from coarse pink and heterogeneous granites show results close to normal distribution. In histograms, values below the average are generally dense, and values above the average are few and are obtained discretely (Figure 3). The reason for this may be the inhomogeneity of the mineral distribution in the measured rocks and the insufficient number of measurements.

DISCUSSION

Gridded susceptibility as well as the conductivity values obtained using 22 sites on the northern side of the Horseshoe Island are illustrated in Figures 4 and 5. The results obtained are discussed below, respectively, taking into account the lithological, pollution and vertical variations.

Magnetic Susceptibility and Conductivity Values vs Lithological Variance

Since approximately 66% of the island is covered with snow and ice, the boundaries of the geological units that can be distinguished according to the outcropping rocks are also given in Figure 2 [24]. A generally similar northeast-southwest trend is observed both in the unit boundaries on the geological map and the magnetic susceptibility and conductivity results (Figures 4 and 5). Because rock outcrops are covered in most places, measurement points are limited, and measurements are generally made from similar granitic rock variations (except, gabbro and granitic gneiss), general transition trends could be determined rather than determining more precise lithological variances. Limited time on the island, difficulty in reaching some areas due to ice, and transportation problems of rock samples posed obstacles to sampling. Despite the limited number of samplings, distinctive results were obtained for different rock lithology (Table 1). However, increasing the sample locations (aside from the limitations mentioned above) would naturally make the results more statistically reliable.

Spatial Distribution of the Susceptibility and Conductivity Variation

In the gridded images of the results, high and low value zones are obvious for both measurements. Magnetic susceptibility results were calculated to be highest in the Sally Cove region where the HSM No:63 is located and relatively lowest in the Gaul Cove region (Figure 1c). The Turkish Scientific Station (TARS) (Figure 1d) demarcates the northeast-southwest oriented high to low switching zone of magnetic susceptibility (Figure 4 and 5). It is especially important in terms of pollution that the highest values of magnetic susceptibility are obtained around the HSM No:63. In the conductivity maps, data almost opposite to the magnetic susceptibility results were obtained. While high conductivity values dominates around the Gaul Cove and north of Lystad Bay, low conductivity values were acquired around Sally Cove. Once again, the region where the TARS is located constitutes a turning point in terms of conductivity changes. Both data sets have relatively low frequency content. Therefore, in gridded maps, more general trends are distinct rather than high-frequency abrupt changes (Figure 4 and 5). Although the results show significant differences depending on the lithology (Table 1 and Figure 3), the dominance of low frequency is due to limited sampling.

Correlation Between Vertical Penetration of Possible Pollution and Rock Mineral Impact

In order to ensure consistency of results and eliminate possible anisotropic effects, both measurements were performed from two different sides of a sample. There are large similarities in the images of the results obtained from two different sides of each sample (Figures 4 and 5). In addition, it was aimed to reveal possible surface pollutant effects by taking measurements in a certain order (1 cm) in the vertical direction. In the maps obtained from the averages of the top and bottom measurement results, largely similar results were obtained rather than significant differences due to possible pollutants (Figure 6). In addition, since the study area is located in an area far from anthropological pollutant effects and is surrounded by the sea, it could be expected that possible pollutant effects would be concentrated in coastal areas, carried by water rather than from the interior of the island. No such anomaly is observed along the coast in both susceptibility and conductivity values. Only at Sally Cove, where the HSM No:63 is located, is there a significant high susceptibility and very low conductivity values.

These results are suppressed by the extreme values obtained from the gabbro samples at locations Hrsh 9 and Hrsh 22. By taking extra measurements from other lithological rock (except Gabbro) around the HSM No:63, where the possible polluting effect can be observed at the highest rate due to constructions for research purposes (late 1950s) and living requirements, it can be more clearly demonstrated whether the values are due to polluting effects or the mineral composition within the rock. However, according to the data we have, pollution-based effects cannot be revealed according to maps, both vertically and spatially (especially in coastal areas). Thus, the obtained grid maps probably reveal lithology-based mineral variations. There is no significant change, especially in terms of the differences between the data obtained from the highest and lowest levels. Although there are nearly uniform spatial distributions in the two analyses, the small differences in coastal areas high probably related to the remote areas from the sample locations and the spurious effects of gridding (Figure 6).

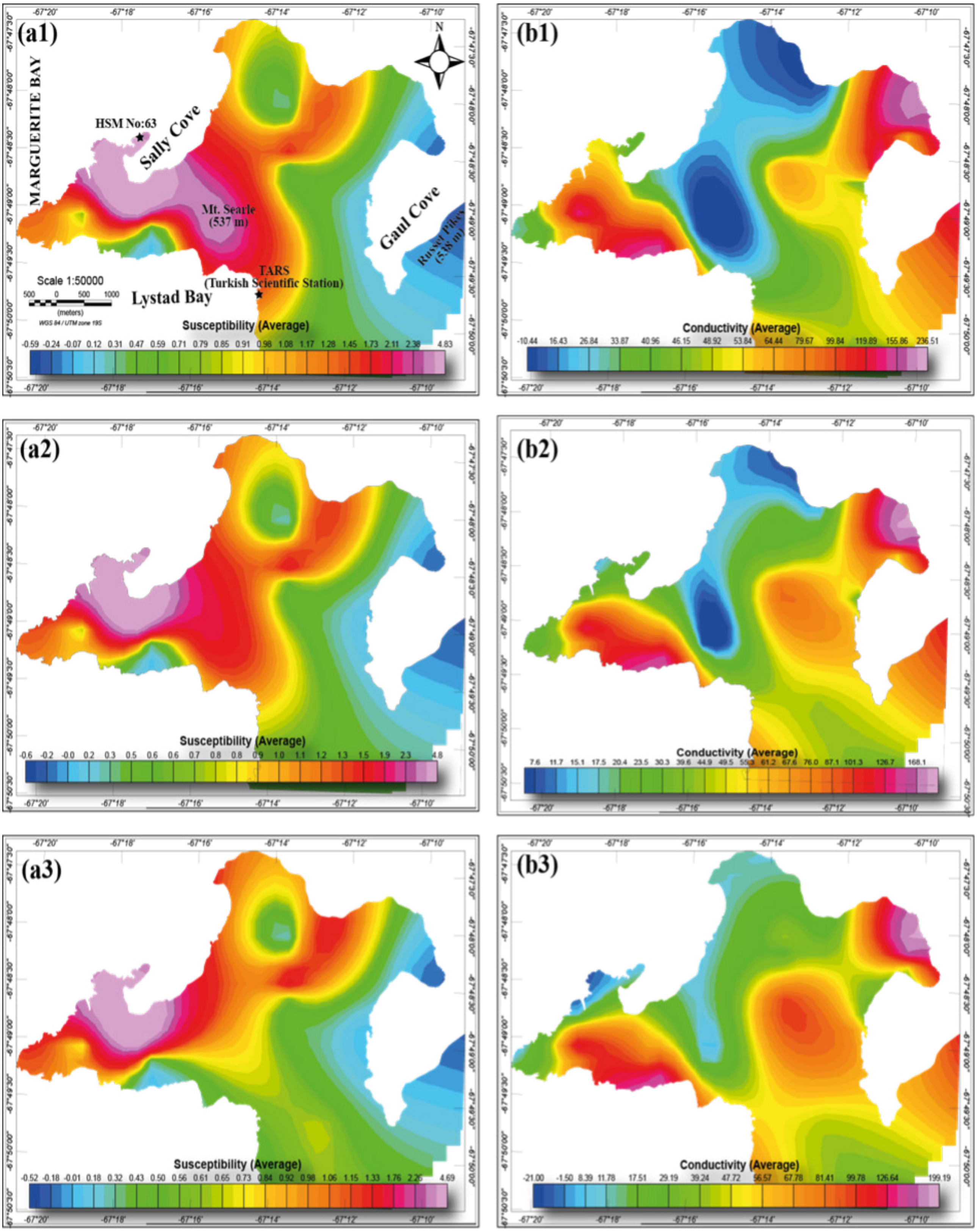

Figure 4. Gridding of magnetic susceptibility and conductivity results (side-1) obtained from 22 different sample locations. Sample locations are given in Figure 2a

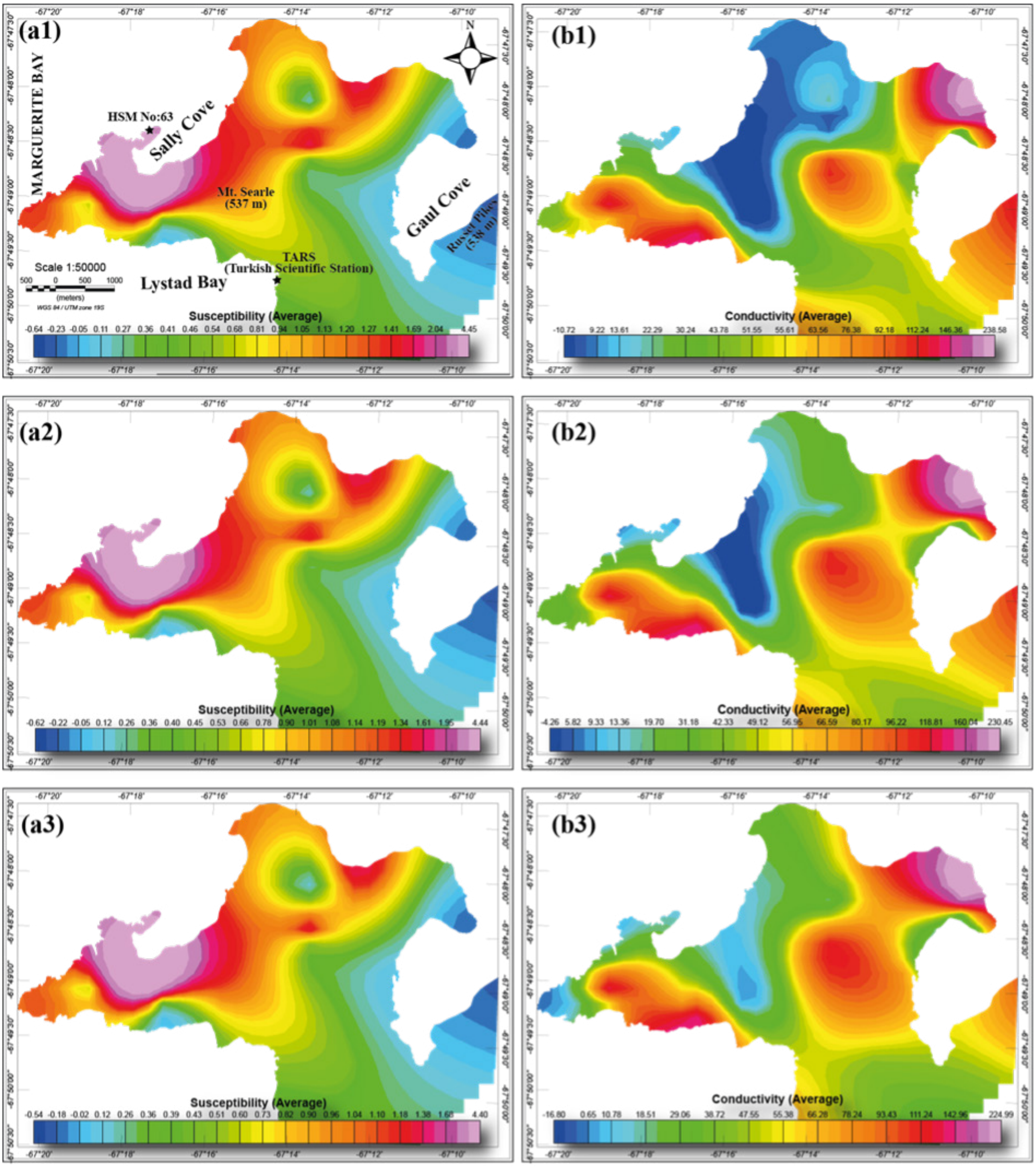

Figure 5. Gridding of magnetic susceptibility and conductivity results (side-2) obtained from 22 different sample locations

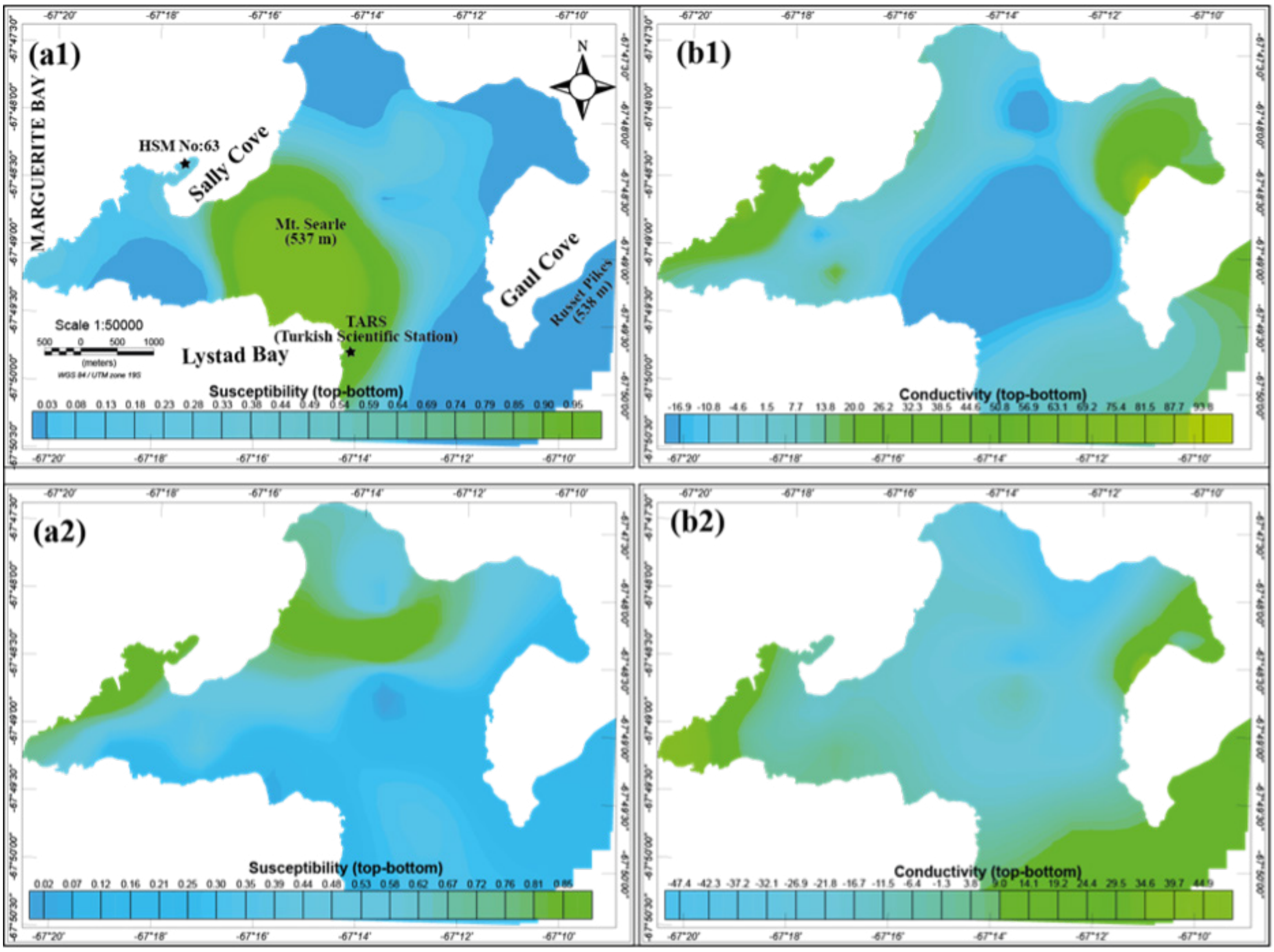

Figure 6. Subtracted results of the top from bottom values of the gridded magnetic susceptibility and conductivity measurements

CONCLUSIONS

Based on the measurement of magnetic susceptibility and conductivity in basement rocks collected from Horseshoe Island, Antarctica, the spatial distribution of susceptibility and conductivity, and the correlation between lithological variances, pollution aspect were discussed. Key findings include:

(1)Magnetic susceptibility and conductivity provided distinctive values for different rock lithologies.

(2)Geological boundaries were inferred based on susceptibility and conductivity trends but remained imprecise due to limited sampling.

(3)High and low anomaly zones were identified, with a distinct anomaly near HSM No:63 potentially linked to construction-related pollution.

(4)No significant differences were observed between surface and depth measurements, indicating a stronger influence of mineral content over pollution.

Future studies with more detailed sampling and analysis could better elucidate the relationship between the observed anomalies and pollution effects.

ACKNOWLEDGEMENT

This study was carried out under the auspices of the Presidency of the Republic of Türkiye, supported by the Ministry of Industry and Technology (TUBITAK, project no. 122G255), and coordinated by TUBITAK MAM Polar Research Institute. We also to thank KTU Foreign Languages Office for editing our manuscript.

DATA AVAILABILITY STATEMENT

The authors confirm that the data that supports the findings of this study are available within the article. Raw data that support the finding of this study are available from the corresponding author, upon reasonable request.

CONFLICT OF INTEREST

The author declared no potential conflicts of interest with respect to the research, authorship, and/or publication of this article.

USE OF AI FOR WRITING ASSISTANCE

Not declared.

ETHICS

There are no ethical issues with the publication of this manuscript.

REFERENCES

1. P. Yang, J. M. Byrne, H. Li, and H.-B. Shao, 'Evaluation of semi-arid arable soil heavy metal pollution by magnetic susceptibility in the Linfen basin of China', Arid Land Research and Management, vol. 30, no. 3, pp. 258–268, 2016.
2. L. Luo, Y. Ma, S. Zhang, D. Wei, and Y. G. Zhu, 'An inventory of trace element inputs to agricultural soils in China', Journal of Environmental Management, vol. 90, no. 8, 2009, doi: 10.1016/j.jenvman.2009.01.011.
3. V. Hoffmann, M. Knab, and E. Appel, 'Magnetic susceptibility mapping of roadside pollution', Journal of Geochemical Exploration, vol. 66, no. 1–2, 1999, doi: 10.1016/S0375-6742(99)00014-X.
4. M. Rachwał, K. Kardel, T. Magiera, and O. Bens, 'Application of magnetic susceptibility in assessment of heavy metal contamination of Saxonian soil (Germany) caused by industrial dust deposition', Geoderma, vol. 295, 2017, doi: 10.1016/j.geoderma.2017.02.007.
5. Menshov, O., Vyzhva, S., Horoshkova, L., Tonkha, O., Ivanik, O., Pereira, P., Dindaroglu, T., Pastushenko, T., Eiben, H. 'Distribution of soil magnetic susceptibility as a pollution indicator in the urban and tourist city of Lviv, Ukraine', Environ Earth Sci, vol. 82, no. 21, 2023, doi: 10.1007/s12665-023-11176-8.
6. A. Schmidt, R. Yarnold, M. Hill, and M. Ashmore, 'Magnetic susceptibility as proxy for heavy metal pollution: A site study', Journal of Geochemical Exploration, vol. 85, no. 3, 2005, doi: 10.1016/j.gexplo.2004.12.001.
7. M. A. E. Chaparro, H. Nuñez, J. M. Lirio, C. S. G. Gogorza, and A. M. Sinito, 'Magnetic screening and heavy metal pollution studies in soils from Marambio Station, Antarctica', Antarctic Science, vol. 19, no. 3, 2007, doi: 10.1017/S0954102007000454.
8. T. Magiera, Z. Strzyszcz, A. Kapicka, and E. Petrovsky, 'Discrimination of lithogenic and anthropogenic influences on topsoil magnetic susceptibility in Central Europe', Geoderma, vol. 130, no. 3–4, 2006, doi: 10.1016/j.geoderma.2005.02.002.
9. M. Hanesch and R. Scholger, 'Mapping of heavy metal loadings in soils by means of magnetic susceptibility measurements', Environmental Geology, vol. 42, no. 8, 2002, doi: 10.1007/s00254-002-0604-1.
10. T. Özkaptan, A. E. Babacan, and M. Özkaptan, 'Geophysical and morphological constraints on active tectonics in the Eastern Pontides (Turkey)', Tectonophysics, vol. 843, 2022, doi: 10.1016/j.tecto.2022.229620.
11. Maus, S., Barckhausen, U., Berkenbosch, H., Bournas, N., Brozena, J., Childers, V., Dostaler, F., Fairhead, J. D.,Finn, C.,von Frese,R.R.B.,Gaina,C.,Golynsky,S.,Kucks, R.,Lühr, H.,Milligan,P.,Mogren,S.,Müller,R.D.,Olesen,O.,Pilkington,M.,Saltus,R.,Schreckenberger, B., Thébault, E.,Caratori Tontini, F. 'EMAG2: A 2–arc min resolution Earth Magnetic Anomaly Grid compiled from satellite, airborne, and marine magnetic measurements', Geochemistry, Geophysics, Geosystems, vol. 10, no. 8, doi: 10.1029/2009GC002471.
12. B. Meyer, R. Saltus, and A. Chulliat, 'EMAG2v3: Earth Magnetic Anomaly Grid (2-arc-minute resolution)', NOAA National Centers for Environmental Information. [Online]. Available: https://doi.org/10.7289/V5H70CVX
13. D. Jordanova, L. Veneva, and V. Hoffmann, 'Magnetic susceptibility screening of anthropogenic impact on the Danube river sediments in Northwestern Bulgaria - Preliminary results', Studia Geophysica et Geodaetica, vol. 47, no. 2, 2003, doi: 10.1023/A:1023736111156.
14. S. G. Lu, S. Q. Bai, and Q. F. Xue, 'Magnetic properties as indicators of heavy metals pollution in urban topsoils: A case study from the city of Luoyang, China', Geophys J Int, vol. 171, no. 2, 2007, doi: 10.1111/j.1365-246X.2007.03545.x.
15. T. Yang, Q. Liu, L. Chan, and G. Cao, 'Magnetic investigation of heavy metals contamination in urban topsoils around the East Lake, Wuhan, China', Geophysical Journal International, vol. 171, no. 2, 2007, doi: 10.1111/j.1365-246X.2007.03558.x.
16. Morton-Bermea, O., Hernandez, E., Martinez-Pichardo, E., Soler-Arechalde, A. M., Santa-Cruz,R.L., Gonzalez-Hernandez, G., L. Beramendi-Orosco, Urrutia-Fucugauchi, J. ,'Mexico City topsoils: Heavy metals vs. magnetic susceptibility', Geoderma, vol. 151, no. 3–4, 2009, doi: 10.1016/j.geoderma.2009.03.019.
17. Ö. Makaroglu, 'Küçükçekmece Lagünü'nün Çevre Manyetizması: Son 3900 yıl boyunca paleo-ortam değişimleri', Journal of Advanced Research in Natural and Applied Sciences, vol. 9, no. 3, pp. 545–559, 2023.
18. M. El Baghdadi, A. Barakat, M. Sajieddine, and S. Nadem, 'Heavy metal pollution and soil magnetic susceptibility in urban soil of Beni Mellal City (Morocco)', Environmental Earth Sciences, vol. 66, no. 1, 2012, doi: 10.1007/s12665-011-1215-5.

19. R. Kandemir, Y. Demir, C. Şen, and U. C. Yağcioğlu, 'The petrogenesis of analcime in the Coppermine Formation on Robert Island, South Shetland Islands, Antarctica', Turkish Journal of Earth Sciences, vol. 32, no. SI-8, 2023, doi: 10.55730/1300-0985.1886.
20. N. S. Ergüven, B. Özsoy, S. Yirmibeşoğlu, and Ö. Oktar, 'Regulation of Mineral Resource Activities in Antarctica', International Journal of Environment and Geoinformatics, vol. 9, no. 2, 2022, doi: 10.30897/ijegeo.907991.
21. R. G. B. Renner, 'British Antartic Survey Scientific Reports: No.77, Gravity and Magnetic Surveys in Grahan Land', 1980.
22. C. Yıldırım, A. Çiner, M. A. Sarıkaya, and A. Hidy, 'Cosmogenic surface exposure (10Be) dating of raised beaches in Marguerite bay, Antarctic Peninsula: Implications for relative sea-level history', Quaternary Science Reviews, vol. 344, p. 108995, Nov. 2024, doi: 10.1016/J.QUASCIREV.2024.108995.
23. C. Yıldırım, 'Geomorphology of Horseshoe Island, Marguerite Bay, Antarctica', Journal of Maps, vol. 16, no. 2, 2020, doi: 10.1080/17445647.2019.1692700.
24. D. W. Matthews, 'The geology of Horseshoe and Lagotellerie Islands, Marguerite Bay, Graham Land.', British Antarctic Survey Bulletin, vol. 52, 1983.
25. M. R. A. Thomson, R. J. Pankhurst, and P. D. Clarkson, 'The Antarctic Peninsula - a Late Mesozoic-Cenozoic arc (review).', Antarctic earth science. 4th international symposium, 1983.
26. B. C. Storey and S. W. Garrett, 'Crustal growth of the Antarctic Peninsula by accretion, magmatism and extension', Geological Magazine, vol. 122, no. 1, 1985, doi: 10.1017/S0016756800034038.
27. I. L. Millar, R. J. Pankhurst, and C. M. Fanning, 'Basement chronology of the Antarctic Peninsula: Recurrent magmatism and anatexis in the Palaeozoic Gondwana margin', Journal of the Geological Society, vol. 159, no. 2, 2002, doi: 10.1144/0016-764901-020.
28. A. P. M. Vaughan, C. D. Wareham, and I. L. Millar, 'Granitoid pluton formation by spreading of continental crust: The Wiley Glacier complex, northwest Palmer Land, Antarctica', Tectonophysics, vol. 283, no. 1–4, 1997, doi: 10.1016/S0040-1951(97)00150-9.
29. S. Yirmibeşoğlu, Ö. Oktar, and B. Özsoy, 'Review of Scientific Research Conducted in Horseshoe Island Where Potential Place for Turkish Antarctic Base', International Journal of Environment and Geoinformatics, vol. 9, no. 4, 2022, doi: 10.30897/ijegeo.1018913.